



## Sprouty2 regulates endochondral bone formation by modulation of RTK and BMP signaling



Adriane Joo<sup>a,b,1</sup>, Roger Long<sup>c,1</sup>, Zhiqiang Cheng<sup>d</sup>, Courtney Alexander<sup>a,b</sup>,  
Wenhan Chang<sup>b,d</sup>, Ophir D. Klein<sup>a,b,c,e,\*</sup>

<sup>a</sup> Department of Orofacial Sciences, University of California, San Francisco, San Francisco, CA, United States

<sup>b</sup> Program in Craniofacial Biology, University of California, San Francisco, San Francisco, CA, United States

<sup>c</sup> Department of Pediatrics, University of California, San Francisco, San Francisco, CA, United States

<sup>d</sup> Endocrine Research Unit, Department of Veterans Affairs Medical Center, Department of Medicine, University of California, San Francisco, San Francisco, CA, United States

<sup>e</sup> Institute for Human Genetics, University of California, San Francisco, San Francisco, CA, United States

### ARTICLE INFO

#### Article history:

Received 24 January 2016

Revised 21 April 2016

Accepted 24 April 2016

Available online 26 April 2016

#### Keywords:

Endochondral bone formation

Chondrocytes

FGFs

BMPs

Sprouty

### ABSTRACT

Skeletal development is regulated by the coordinated activity of signaling molecules that are both produced locally by cartilage and bone cells and also circulate systemically. During embryonic development and postnatal bone remodeling, receptor tyrosine kinase (RTK) superfamily members play critical roles in the proliferation, survival, and differentiation of chondrocytes, osteoblasts, osteoclasts, and other bone cells. Recently, several molecules that regulate RTK signaling have been identified, including the four members of the Sprouty (Spry) family (*Spry1–4*). We report that *Spry2* plays an important role in regulation of endochondral bone formation. Mice in which the *Spry2* gene has been deleted have defective chondrogenesis and endochondral bone formation, with a postnatal decrease in skeletal size and trabecular bone mass. In these constitutive *Spry2* mutants, both chondrocytes and osteoblasts undergo increased cell proliferation and impaired terminal differentiation. Tissue-specific *Spry2* deletion by either osteoblast- (*Col1-Cre*) or chondrocyte- (*Col2-Cre*) specific drivers led to decreased relative bone mass, demonstrating the critical role of *Spry2* in both cell types. Molecular analyses of signaling pathways in *Spry2*<sup>-/-</sup> mice revealed an unexpected upregulation of BMP signaling and decrease in RTK signaling. These results identify *Spry2* as a critical regulator of endochondral bone formation that modulates signaling in both osteoblast and chondrocyte lineages.

© 2016 Elsevier Inc. All rights reserved.

### 1. Introduction

Chondrogenesis is an essential intermediate step in endochondral ossification through which long bones and vertebrae are formed. Endochondral bone formation begins when mesenchymal cells migrate, condense at the sites of future skeletal structures, and commit to the chondrocytic lineage. Subsequent proliferation of chondrocytes leads to expansive linear growth and enlargement. Eventually, chondrocytes stop proliferating and begin to undergo hypertrophy at the center of the cartilaginous anlage, which lays the foundation for future ossification. The hypertrophic chondrocytes regulate reorganization and mineralization of the extracellular matrix (ECM) and subsequent invasion of vasculature that brings in precursors of various bone cells. The

latter cells in turn mediate the osteogenic phase of endochondral bone formation [1].

Endochondral bone formation is tightly regulated by a complex system of signaling networks and feedback mechanisms controlled by local paracrine factors and systemic hormones. These factors include BMPs, FGFs, Wnts, hedgehog proteins, and insulin-like growth factor-1 (IGF-1). The spatiotemporal expression and relative concentration of these signaling factors within and around the growth plate (GP) are coordinated to regulate an orderly initiation and progression of proliferation, hypertrophy, and terminal differentiation of growth plate chondrocytes (GPCs) and osteoblasts (OBs) [1,2]. Disruptions in any of these steps result in cartilage and/or bone defects.

Sprouty (Spry) was identified in *Drosophila* as an inhibitor of *breathless*, the fly equivalent of the FGF receptor [3]. Four orthologs (*Spry1–4*) of *Drosophila Spry* (*dSpry*) have been identified in mammals, and *Spry2* exhibits the highest homology to *dSpry* [4–6]. Sprouty gene products have been reported to function as both negative and positive regulators of MAPK signaling downstream of various receptor tyrosine kinase (RTK) signaling cascades in a cell type- and context-dependent manner. The SPRY2 protein inhibits MAPK activation induced by FGF, PDGF, and

\* Corresponding author at: Department of Orofacial Sciences, University of California, San Francisco, San Francisco, CA, United States.

E-mail address: [ophir.klein@ucsf.edu](mailto:ophir.klein@ucsf.edu) (O.D. Klein).

<sup>1</sup> Co-first authors.

VEGF, but its effect is thought to be agonistic in signaling downstream of the epidermal growth factor (EGF) receptor [7–9]. *Spry2* has been shown to regulate a number of developmental processes, including limb formation [4], lung branching [5], tooth morphogenesis [10], and kidney development [11]. Because FGF and other RTK family members play a critical role during endochondral bone formation [12,13], we set out to determine if *Spry2* functions in this process.

## 2. Materials and methods

### 2.1. Mouse lines

Mouse lines carrying the *Spry1<sup>tm1.1Jdl</sup>* (*Spry1<sup>-/-</sup>*) [14], *Spry2<sup>tm1.1Mrt</sup>* (*Spry2<sup>-/-</sup>*) [15], *Spry4<sup>tm1.2Mrt</sup>* (*Spry4<sup>-/-</sup>*) [10], and *Spry2<sup>tm1Mrt</sup>* (*Spry2<sup>fllox</sup>*) alleles [15], as well as the Tg(*Col1a1-cre*)2Bek (*Col1-Cre*) [16], and Tg(*Col2a1-cre*)1Bhr (*Col2-Cre*) transgenes [17] were maintained in the CD-1 mixed background and genotyped as previously described. Conditional inactivation of *Spry2* was achieved by crossing *Spry2<sup>fllox/fllox</sup>* females [15] with either *Col1-Cre<sup>Tg/+</sup>*; *Spry2<sup>+/-</sup>* males [16] for OB-specific KO (*Col1-Cre*; *Spry2<sup>fllox/-</sup>*) or *Col2-Cre<sup>Tg/+</sup>*; *Spry2<sup>+/-</sup>* males [17] for chondrocyte-specific KO (*Col2-Cre*; *Spry2<sup>fllox/-</sup>*) and genotyped as previously described. Embryos and pups from timed mating and adult male mice were studied as described in the protocols reviewed and approved by the IACUC of the University of California, San Francisco (UCSF). All animal experiments have been carried out in accordance with the National Institutes of Health guide for the care and use of Laboratory animals. All mice were housed in temperature and humidity controlled rooms in animal care facilities overseen by the UCSF Laboratory Animal Resource Center (LARC), which is accredited by the Association and Accreditation of Laboratory Animal Care (AAALAC).

### 2.2. mRNA *in situ* hybridization

For mRNA *in situ* hybridization, hindlimbs were collected, fixed overnight in 4% paraformaldehyde at 4 °C, and decalcified for 3 days in either 10% EDTA for E16.5 embryos or in Morse's solutions for 6-week-old males at 4 °C. Decalcified bones were embedded in paraffin, and sectioned at 7 μm thickness. For traditional mRNA *in situ* detection, anti-sense DIG-labeled RNA probes were generated from plasmids containing fragments of *Spry1*, *Spry2*, and *Spry4*. Section *in situ* hybridization was performed according to standard protocols.

For RNAscope mRNA *in situ* detection, the RNAscope 2.5 High Definition (HD) RED assay kit (Advanced Cell Diagnostics, Inc., Hayward, CA) was used according to the manufacturer's recommendation. Images were captured with a Leica DFC500 microscope using Leica Application Suite (version 4.0.0) program.

### 2.3. Primary GPC culture

Epiphyseal GPs from P2–P4 *Spry2* WT or KO pups were dissected free of soft tissues, and GPCs were released by enzymatic digestion and cultured as described [18]. Proliferation was assessed using BrdU ELISA kit (Cell Signaling Tech., Danvers, MA) following the manufacturer's instructions. Gene expression in GPCs was studied using qPCR.

### 2.4. Primary OB cultures

For primary calvarial OB cultures, calvaria were dissected from CO<sub>2</sub>-euthanized P7–P9 pups, washed in PBS, and sequentially digested in a mixture of 1.5 U/ml collagenase P and 0.05% trypsin. Isolated cells were dispersed into a single-cell suspension and plated in primary medium (DMEM containing 10% FBS, 100 U/ml penicillin/streptomycin, and 0.25 μg/ml fungizone).

To measure cellular proliferation, 5000 calvarial OBs were seeded into each chamber of an 8-chamber slide. Proliferating cells were incubated with BrdU solution (1 mg/ml; Sigma-Aldrich, St. Louis, MO) for 30 min in a 37 °C incubator to facilitate incorporation of BrdU into the newly synthesized DNA of replicating cells. Incorporated BrdU was detected with anti-BrdU Ab (Abcam, Cambridge, MA) and visualized chromogenically with the Liquid DAB+ kit (Dako, Glostrup, Denmark). Images were captured with a Leica DFC500 microscope using Leica Application Suite (version 4.0.0) program. Both BrdU-labeled cells and unlabeled cells within each chamber were manually counted, and the percentage of BrdU-labeled cells against the total cell population was calculated.

Bone marrow osteoprogenitor cells were harvested and induced for differentiation as described previously [19] except cells were plated at  $2 \times 10^5$  cells/well in 6-well plates. At day 14 of induction, cells were stained for alkaline phosphatase activity using the alkaline phosphatase, leukocyte kit (procedure no. 86; Sigma-Aldrich, St. Louis, MO) following the manufacturer's instructions. At day 28 of culture, calcified nodules were stained with alizarin red as described previously [19]. The number of alkaline phosphatase- or alizarin red-positive colonies was calculated as the percentage of stained cells/total plated area. Measurement was done using ImageJ ( $n = 4$ ).

### 2.5. Quantitative PCR

For qPCR analysis, RNA was extracted from either primary GP chondrocytes or primary calvarial OBs using the RNeasy mini kit (Qiagen, Hilden, Germany) according to the manufacturer's instructions. Expression levels of Sprouty genes were measured using the GoTaq qPCR Master Mix (Promega, Madison, WI) with a Mastercycler Realplex (Eppendorf, Hamburg, Germany). RNA levels were normalized to *L19*, which encodes a ribosomal protein, and displayed as percent of expression. Sequences are available upon request.

### 2.6. Analyses of growth and skeletal phenotype in mice

At 4 or 6 weeks of age, *Spry2<sup>-/-</sup>*, *Col1-Cre*; *Spry2<sup>fllox/-</sup>*, or *Col2-Cre*; *Spry2<sup>fllox/-</sup>* males and their control littermates were weighed individually prior to CO<sub>2</sub> euthanasia. Both femurs and tibias were collected from 4- and 6-week-old male mice and their control littermates free of soft tissues, fixed in 10% neutral buffered formalin (NBF, 10% formalin in PBS) overnight, and stored in 70% ethanol. Bone length of both femurs and tibias was recorded by measuring the longest distance between two epiphyses with a caliper.

### 2.7. MicroCT (μCT) scans of long bones

Femurs were isolated from 6-week-old *Spry1<sup>-/-</sup>*, *Spry2<sup>-/-</sup>*, *Spry4<sup>-/-</sup>*, *Col1-Cre*; *Spry2<sup>fllox/-</sup>* or *Col2-Cre*; *Spry2<sup>fllox/-</sup>* males and their control littermates, fixed in 10% NBF overnight, and stored in 70% ethanol. Distal femurs were scanned to analyze microarchitectural structures of Trabecular (Tb) bones on a SCANCO vivaCT 40 scanner (SCANCO Medical, Basserdorf, Switzerland) with 10.5 μm voxel size and 55 kV X-ray energy, as per Boussein et al. [20]. For Tb bone, 100 serial cross-sectional scans (1.05 mm) were obtained from the end of the GP extending proximally. A threshold of 300 mg hydroxyapatite (HA)/mm<sup>3</sup> was applied to segment total mineralized bone matrix from soft tissue. Image analysis and 3D reconstructions were performed with the manufacturer's software (SCANCO Medical AG, Bassersdorf, Switzerland) by the SF-VAMC Bone Imaging Core facilities.

### 2.8. Histomorphometric analyses of Tb bones

To study adult bones, femurs were isolated from 6-week-old *Spry2<sup>-/-</sup>* and WT littermate males, fixed overnight in 10% NBF, dehydrated with ethanol, defatted with xylene, and embedded in

MMA (Sigma-Aldrich, St. Louis, MO). Adjacent sections (5 or 10  $\mu\text{m}$  in thickness) were cut on an automated microtome (LEICA RM2255, Germany) and mounted on gelatin-coated slides for various staining procedures. Digital images of stained bone sections were acquired. For histomorphometry, the region of interest began approximately 150  $\mu\text{m}$  below the femoral GP, extended 1 mm distally and flanked the two sides that are 100  $\mu\text{m}$  apart from cortical bone. Two sections (approximately 50–100  $\mu\text{m}$  apart) per bone sample were analyzed for each staining method, and the average was used for statistical analyses. The histomorphometric analysis was done by the SF-VAMC Bone Imaging Core. The terminology and units used are those recommended by the Histomorphometry Nomenclature Committee of the American Society for Bone and Mineral Research [21].

The von Kossa (VK) staining method was performed to detect the phosphate-containing minerals and calculate static bone parameters: Tb.BV/TV, Tb.N, and Tb.Sp. To quantify structural parameters of OC-positive resorbing surface, sections were stained with TRAP reagents. The deduced indices include ES/BS, N.Oc/BS, and N.Oc/ES.

For dynamic bone formation indices, calcein (15 mg/kg body weight) and xylenol orange (15 mg/kg body weight) were administered sequentially to both control and experimental groups at 14 and 7 days before sample collection, respectively. Unstained MMA-embedded bone sections were obtained as described above and used to quantify MS/BS, MAR, and BFR/BS. Bone images were acquired by Zeiss AXIO Imager M1 Microscope with an automated stage and analyzed using BioQuant OSTEO 2009 software (Version 9.00, BIOQUANT Image Analysis Co., Nashville, TN).

### 2.9. Histological, histomorphometric, and immunohistological analyses of GP cartilage

To study GP cartilage in embryonic limbs, E18.5 hindlimbs were collected from both *Spry2*<sup>-/-</sup> and WT littermate embryos, cleaned of soft tissues, and fixed prior to embedding in glycol methacrylate (GMA). GMA-embedded limbs were sectioned at 2.5  $\mu\text{m}$  thickness and stained using the VK with Safranin-O (SaFO) reagents. Average numbers of chondrocytes within the proliferative zone were calculated by manually counting cells within randomly selected four 1 in.  $\times$  1 in. grids per sample and averaging total number of cells within each grid. The average height of the hypertrophic zone was calculated by measuring the distance between top row of hypertrophic chondrocytes and chondroosseous junctions at 10 different locations along the width of the GP.

For immunohistochemistry, hindlimbs were processed in the same fashion as samples for *in situ* hybridization except that decalcification was done in 10% EDTA for all specimens. Sections were probed with commercially available antibodies against phospho-MEK1/2 and phospho-SMAD1/5/8 (Cell Signaling Tech., Danvers, MA).

For the BrdU cell proliferation and TUNEL analyses, pregnant dams with E18.5 embryos were injected with BrdU solution (50 mg/g body weight; Sigma-Aldrich, St. Louis, MO) 2 h prior to euthanasia. BrdU-incorporated chondrocytes in limb sections were detected with anti-BrdU antibody (Abcam, Cambridge, MA). Bound antibody was visualized chromogenically with the Liquid DAB+ kit (Dako, Glostrup, Denmark). Apoptotic cells in embryonic limb sections were detected with the *in situ* cell death detection kit, TMR red (Roche, Indianapolis, IN) according to the manufacturer's instructions.

To quantitate cellular proliferation, four 1 in.  $\times$  1 in. grids were randomly selected from each image and numbers of BrdU-labeled cells and unlabeled cells within each grid were obtained to calculate the percentage of BrdU-labeled cells against the total cell numbers.

### 2.10. Statistical analysis

All experiments were performed independently at least three times, and data were presented as mean  $\pm$  SD. Student's *t*-test was used to determine *p* values and *p* < 0.05 was deemed to be significant.

## 3. Results

### 3.1. *Spry1*, *Spry2*, and *Spry4* are expressed in both cartilage and bone cells

To determine the mRNA expression pattern of the Sprouty gene family, *in situ* hybridization analysis was performed on long bones of E16.5 and 6-week-old CD1 mice. *Spry1*, *Spry2*, and *Spry4* RNA transcripts were detected in the proliferating, prehypertrophic, and hypertrophic chondrocytes in the embryonic (Fig. 1A–C') and postnatal GPs (Fig. 1D–F), and in the OBs and osteoclasts (OCs) in the primary and secondary spongiosa (Fig. 1D'–F'). *Spry3* mRNA was not detected in these tissues (data not shown).

Quantitative PCR analyses of cultured GPCs (Supplementary Fig. 1A–C) and calvarial OBs (Supplementary Fig. 1D–F) confirmed the expression of *Spry1*, *Spry2*, and *Spry4* RNA and the lack of expression of *Spry3* RNA (data not shown) in these cells. As expected, *Spry2* mRNA expression was not detected in GPCs and OBs isolated from the *Spry2*<sup>-/-</sup> mice (Supplementary Fig. 1B and E). Interestingly, the expression of *Spry1* and *Spry4* was upregulated significantly in the *Spry2*<sup>-/-</sup> mice (Supplementary Fig. 1A, C, D, F), suggesting a compensatory increase in expression of these genes in the absence of *Spry2*.

### 3.2. *Spry2*<sup>-/-</sup> mice are smaller and have stunted postnatal skeletal growth

Although the Sprouty genes share a similar expression pattern in long bones, only the *Spry2* KO mice showed growth retardation and a skeletal phenotype (Fig. 2A, B, and Supplementary Fig. 2A); the *Spry1* and *Spry4* mutants were grossly normal in terms of their skeletons (data not shown). While *Spry2*<sup>-/-</sup> pups were indistinguishable from their WT littermates in body weight at birth, their postnatal growth was stunted. By P7, *Spry2*<sup>-/-</sup> pups were significantly smaller than control littermates (Supplementary Fig. 2B), and at 6 weeks of age, their body weight was only 39% of their control littermates (Supplementary Fig. 2C). These growth defects were accompanied by reduction of femur and tibia length, by 14% and 11%, respectively (Supplementary Fig. 2D, E).

### 3.3. *Spry2*<sup>-/-</sup> mice have less trabecular (Tb) bone due to slow bone turnover

In addition to the abnormalities in longitudinal bone growth, we found abnormal microarchitecture of the long bones in *Spry2*<sup>-/-</sup> mice. MicroCT ( $\mu\text{CT}$ ) analyses of the distal femurs showed decreased ratio of Tb bone volume to tissue volume (Tb.BV/TV), Tb number (Tb.N), and Tb thickness (Tb.Th), by 42, 25, and 13%, respectively, and increased Tb spacing (Tb.Sp) by 32% of the *Spry2*<sup>-/-</sup> mice compared to control littermates (Fig. 2C–F). These bone parameters were unchanged in the *Spry1*<sup>-/-</sup> and *Spry4*<sup>-/-</sup> mice (Supplementary Fig. 3), indicating a minimal role for these two genes in skeletal development.

Histomorphometric analyses of undecalcified femurs from 6-week-old *Spry2*<sup>-/-</sup> and control mice supported the  $\mu\text{CT}$  findings. Static histomorphometry with von Kossa (VK)/tetrachrome staining showed a reduced Tb.BV/TV, Tb.N, and Tb.Th, and increased Tb.Sp in the *Spry2*<sup>-/-</sup> bones (Supplementary Fig. 4). The decreased Tb bone mass in the *Spry2*<sup>-/-</sup> mice was likely due to a reduction in bone formation rather than an increase in bone resorption, as the mineral apposition rate (MAR) and bone formation rate (BFR/BS) in the calcein/xylenol orange-labeled femurs were decreased by 26% and 23%, respectively (Fig. 3B,C), and OC numbers (N.Oc/Bs) and bone resorption surface (ES/BS) in tartrate resistant acid phosphatase (TRAP)-stained bone sections were decreased by 23% and 27%, respectively (Fig. 3D,E). The unchanged ratio of mineralizing surface over bone surface (MS/BS; Fig. 3A) further suggested that the decreased mineral apposition rate was likely due to reduced mineralizing function in *Spry2*<sup>-/-</sup> OBs per unit of mineralizing surface. In support of this notion of OB dysfunction, calvarial OBs and bone marrow stromal cells (BMSCs) isolated from

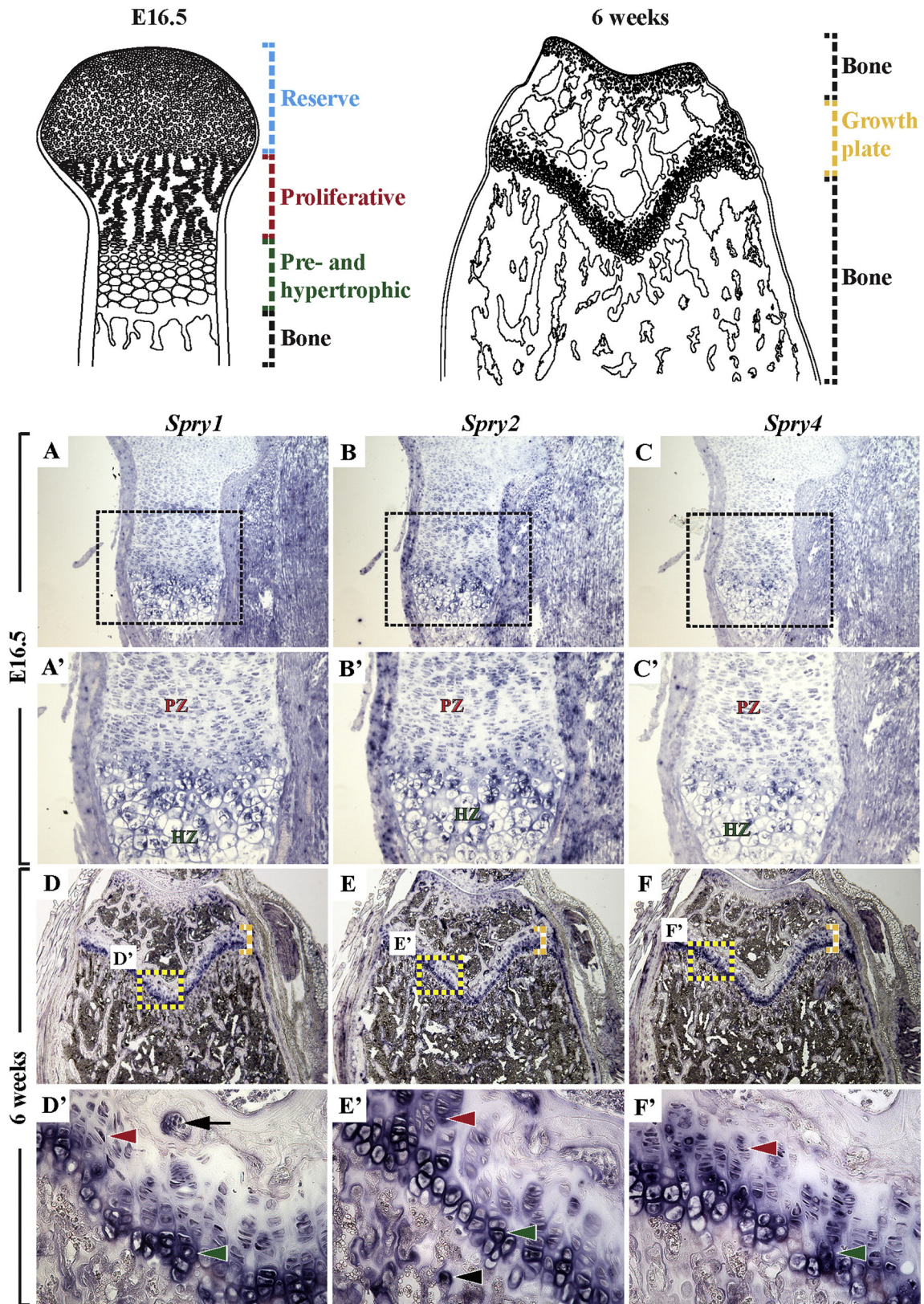


**Fig. 1.** Sprouty gene expression in embryonic and adult long bones. *In situ* hybridization of proximal tibial sections with corresponding RNA probes showing robust expression of *Spry1* (A, A', D, D'), *Spry2* (B, B', E, E'), and *Spry4* (C, C', F, F'), but not *Spry3* (data not shown), in proliferating (red arrowhead), prehypertrophic, and hypertrophic (green arrowhead) chondrocytes in E16.5 embryonic (A–C') and 6-week-old GPs D–F', and in OCs (black arrow) and OBs (black arrowhead) in the primary spongiosa D–F' of WT mice. Top schematic panels: Blue dashed lines – reserve chondrocytes, red dashed lines – proliferative chondrocytes, green dashed lines – pre- and hypertrophic chondrocytes, black dashed lines – bone, yellow dashed lines – GP. (For interpretation of the references to color in this figure legend, the reader is referred to the web version of this article.)

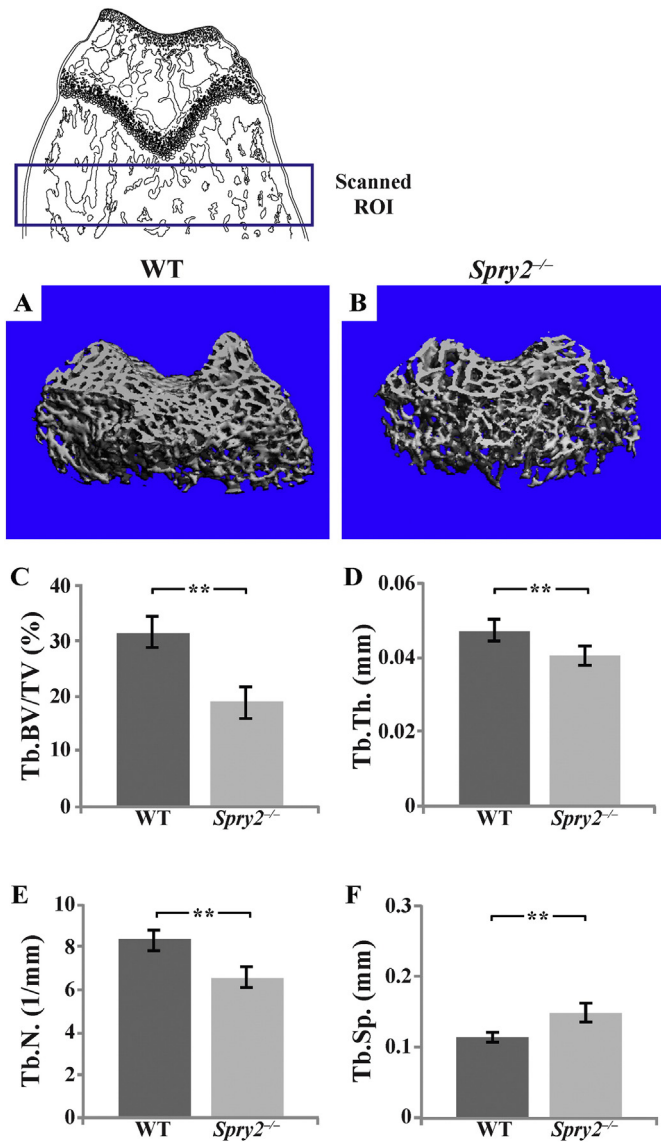


**Fig. 2.** *Spry2*<sup>-/-</sup> mice have less Tb bone.  $\mu$ CT analysis of distal femurs from 6-week-old *Spry2*<sup>-/-</sup> and WT males. 3D reconstructed images of trabecular bones from  $\mu$ CT analysis of WT (A) and *Spry2*<sup>-/-</sup> (B) distal femoral metaphyses (scanned ROI in top schematic panel). (C–F) *Spry2*<sup>-/-</sup> mice have decreased Tb. BV/TV (C,  $p = 0.001$ ), average Tb.Th (D,  $p = 0.002$ ), and Tb.N (E,  $p = 0.001$ ) and increased spacing between trabeculae (F,  $p = 0.001$ ).  $n = 8$  per genotype.

*Spry2*<sup>-/-</sup> mice had a higher rate of proliferation as assessed by BrdU incorporation (Fig. 3F–H) but a reduced capacity to form alkaline phosphatase expressing and mineralized colonies (Fig. 3I–L).

#### 3.4. Conditional inactivation of *Spry2* in chondrocytes or OBs partly recapitulates skeletal defects seen in *Spry2*<sup>-/-</sup> mice

To determine whether the skeletal defects in *Spry2*<sup>-/-</sup> mice were due to the loss of *Spry2* in chondrocytes and/or OBs, we generated either chondrocyte- (*Col2*-Cre;*Spry2*<sup>fllox/-</sup>) or OB-specific (*Col1*-Cre;*Spry2*<sup>fllox/-</sup>) KOs of *Spry2*. Unlike *Spry2*<sup>-/-</sup> animals, both *Col2*-Cre;*Spry2*<sup>fllox/-</sup> and *Col1*-Cre;*Spry2*<sup>fllox/-</sup> mice were indistinguishable from their littermate controls in body weight and femur and tibia length at 6 weeks of age (Supplementary Fig. 2F–K). We also analyzed Tb bone in the distal femurs of 6-week-old mice with either chondrocyte- (*Col2*-Cre;*Spry2*<sup>fllox/-</sup>) or OB-specific (*Col1*-Cre;*Spry2*<sup>fllox/-</sup>) inactivation of *Spry2*. Tissue-specific inactivation of *Spry2* in chondrocytes or OBs at early stages of cartilage and

bone development recapitulated, albeit to a lesser extent, the Tb bone defects of global *Spry2* KOs. *Col2*-Cre;*Spry2*<sup>fllox/-</sup> and *Col1*-Cre;*Spry2*<sup>fllox/-</sup> mice had decreased Tb.BV/TV by 23% and 26%, respectively (Fig. 4A,E), in contrast to a 42% reduction in *Spry2*<sup>-/-</sup> mice. The trabeculae of *Col2*-Cre;*Spry2*<sup>fllox/-</sup> mice were significantly thinner in size (Tb.Th) by 7%, fewer in number (Tb.N) by 10%, and with greater spacing (Tb.Sp) by 10% (Fig. 4B–D). There was a similar phenotype in the *Col1*-Cre;*Spry2*<sup>fllox/-</sup> mice, with a significant decrease in Tb.N by 15%, an increase in Tb.Sp by 14%, and a trend towards thinner trabeculae (Fig. 4F–H). The skeletal phenotype in both of the conditional *Spry2* inactivation models shows that *Spry2* expression in both chondrocytes and OBs is vital for optimal trabecular bone formation. The more pronounced phenotype of the global *Spry2* KO suggests that the roles of *Spry2* in chondrocytes and OBs are independent and additive with respect to endochondral bone formation.

#### 3.5. Mechanisms underlying chondrogenic defects in *Spry2*<sup>-/-</sup> mice

In addition to its role in post-natal endochondral bone formation, *Spry2* is involved in the regulation of chondrogenesis. Histological analysis of the GPs of the distal femurs in E18.5 *Spry2*<sup>-/-</sup> embryos demonstrated a 32% increase in the number of proliferating chondrocytes with typical flattened cell morphology (Fig. 5C). In contrast, chondrocyte differentiation was retarded, as evidenced by a 32% decreased length of the hypertrophic zone of the mutant GP (Fig. 5A',B',D). The hypercellularity of the proliferative zone in *Spry2*<sup>-/-</sup> embryos was due to an increase in cell proliferation, as indicated by 34% more BrdU-positive cells in this zone (Fig. 5E–G), but not cell apoptosis, as the number of TUNEL-positive cells in the hypertrophic zones or in the primary spongiosa of *Spry2*<sup>-/-</sup> embryos was unchanged (Fig. 5H,I).

To characterize the molecular changes within the GPCs associated with the abnormalities of chondrogenesis in *Spry2*<sup>-/-</sup> embryos, we assessed the expression of cartilage extracellular matrix molecules that indicate stages of chondrocyte differentiation by immunohistochemical and RNAscope *in situ* hybridization analyses on sections from control and *Spry2*<sup>-/-</sup> embryonic limbs. We observed no change in expression level of either the alpha-1 subunit of the type II collagen (*Col2a1*; *Col2*), a marker of early resting and proliferative chondrocytes, or the alpha-1 subunit of type X collagen (*Col10a1*), a hypertrophic chondrocyte marker encoded by *Col10a1* (*Col10*), in *Spry2*<sup>-/-</sup> specimens (Fig. 6A–D'). However, more *Col2*-expressing cells can be seen in the chondro-osseous junction of *Spry2*<sup>-/-</sup> (Fig. 6B,B') than in that of WT (Fig. 6A,A'). Furthermore, in agreement with the size reduction of the hypertrophic zone of *Spry2*<sup>-/-</sup> embryos (Fig. 5A',B'), the expression of osteopontin (*Opn*), a marker of terminally differentiated hypertrophic chondrocytes, was altered and decreased in mutants (Fig. 6E–F'). These data indicate that chondrocyte proliferation and initial differentiation occur normally in the absence of *Spry2*, but the terminal differentiation of chondrocytes is delayed in *Spry2*<sup>-/-</sup> embryos, and this may contribute to retarded bone growth.

#### 3.6. Aberrant signaling in *Spry2*<sup>-/-</sup> chondrocytes

Since Sproutys have been found to be negative feedback modulators of growth factor (GF)-mediated MAPK activation, we expected that deletion of *Spry2* would augment RTK signaling. However, immunohistochemical analysis of embryonic GPs revealed a significant decrease in the number of phospho-MEK (pMEK) 1/2-positive cells, pointing to a decrease of RTK signaling in the absence of *Spry2* (Fig. 6G–I). In light of this unexpected effect on RTK signaling, we investigated the impact of *Spry2* deletion on other signaling cascades using the more sensitive RNAscope technology. We showed that bones from *Spry2*<sup>-/-</sup> embryos had increased expression of *Bmp2* in the perichondrium and hypertrophic zone and reduced expression of *Noggin*, a BMP antagonist, throughout the GP (Fig. 6K–N'). Consistent with these findings, there was a significant increase in the number of cells staining for phospho-Smad

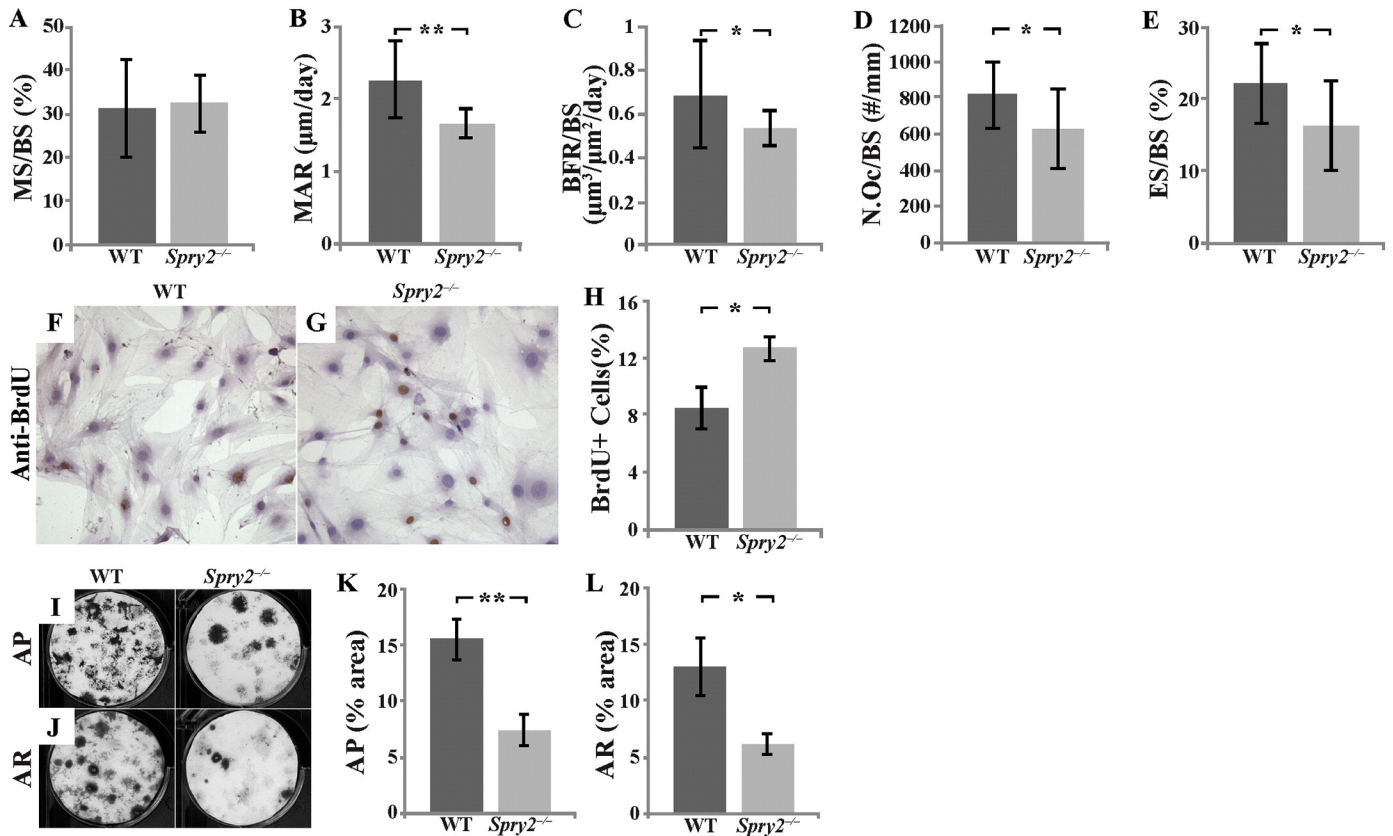


**Fig. 3.** Deletion of *Spry2* leads to slow bone turnover. Trabecular bone formation was assessed by dual fluorochrome labeling ( $n = 14$  for WT and  $n = 14$  for *Spry2*<sup>-/-</sup>). Results showed that MAR (B,  $p = 0.001$ ) and BFR/BS (C,  $p = 0.02$ ) are reduced in 6-week-old *Spry2*<sup>-/-</sup> males without evidence of decreased OB numbers. TRAP staining of distal femurs of 6-week-old *Spry2*<sup>-/-</sup> males showing decreased N.Oc/BS (D,  $p = 0.022$ ) and ES/BS (E,  $p = 0.01$ ). Calvarial OBs from *Spry2*<sup>-/-</sup> mice have increased proliferation as evidenced by increased number of BrdU-positive cells (brown-stained cells) (F–H,  $p = 0.005$ ). Alkaline phosphatase (AP; I, K,  $p = 0.001$ ) and mineralization (AR; J, L,  $p = 0.012$ ) staining of induced BMSCs showing that OB differentiation is delayed or disrupted in *Spry2*<sup>-/-</sup> mice.  $p$ -Values are calculated using the Student's  $t$ -test ( $*p < 0.05$ ,  $**p < 0.005$ ). (For interpretation of the references to color in this figure legend, the reader is referred to the web version of this article.)

(pSMAD)1/5/8, indicating increased BMP signaling (Fig. 6J,O–P'). Previous studies have shown that BMP signaling stimulates *Indian hedgehog* (*Ihh*) expression, which in turn increases expression of *PTHrP* [22,23]. As expected with an increase in BMP signaling, we observed an increase in *Ihh* expression in the *Spry2*<sup>-/-</sup> mice (Fig. 6Q–R'). However, there was no increase in expression of *PTHrP* (Fig. 6S–T'), suggesting an uncoupling between *Ihh* signaling and *PTHrP* expression in the absence of *Spry2*. Thus, in the absence of *Spry2*, the failure of chondrocytes to terminally differentiate is due, at least in part, to increased BMP signaling and decreased RTK signaling.

#### 4. Discussion

We have investigated the role of Sprouty genes during endochondral bone development. *Spry1*, *Spry2*, and *Spry4* were expressed in cartilage and bone, but mice carrying mutant alleles of either *Spry1* or *Spry4* did not manifest any obvious long bone phenotype. In contrast, *Spry2* null mice developed profound postnatal growth and skeletal defects. These observations suggest that only *Spry2* plays a non-redundant role in supporting skeletal development and may explain why upregulation of *Spry1* and *Spry4* in the *Spry2*<sup>-/-</sup> chondrocytes and bone cells was unable to compensate for the loss of *Spry2*. Since defects in the *Spry2* null mice were recapitulated, albeit to a lesser degree, in *Col2*-Cre;*Spry2*<sup>fllox/-</sup> and *Col1*-Cre;*Spry2*<sup>fllox/-</sup> mice, the skeletal defects in *Spry2*<sup>-/-</sup> mice are due, at least in part, to the absence of *Spry2* from chondrocytes and OBs. In contrast to the shortened skeleton in the *Spry2*<sup>-/-</sup> mice, normal bone lengths in *Col2*-Cre;*Spry2*<sup>fllox/-</sup> and *Col1*-Cre;*Spry2*<sup>fllox/-</sup> mice implicate additional actions of *Spry2*, perhaps in

chondro- and/or osteoprogenitors prior, to the activation of *Col2* or *Col1* promoter to support postnatal bone elongation. Alternatively, other *Spry2*-mediated growth signals (local or systemic) may also be needed for complete skeletal development.

Defective GP histology and endochondral bone formation in *Spry2*<sup>-/-</sup> mice indicate a role for *Spry2* during chondrocyte development. This is consistent with our previous report of the requirement of *Spry1* and *Spry2* in proper formation of the temporomandibular joint [24]. The loss of *Spry2* expression does not affect the initiation of chondrogenesis, as limbs of *Spry2*<sup>-/-</sup> mice appear to develop normally until late gestation. Thus, *Spry2* does not significantly impact mesenchymal cell condensation or the subsequent initial differentiation of mesenchymal precursors to chondrocytes. Rather, it regulates chondrocyte proliferation and differentiation, as indicated by the phenotypes in late-gestation *Spry2*<sup>-/-</sup> embryos.

The increased proliferation of the *Spry2*<sup>-/-</sup> GPCs *in vivo* is consistent with previous work showing that increased *Spry2* expression inhibited chondrocyte proliferation in chicks [4]. This hyperproliferative *Spry2*<sup>-/-</sup> phenotype was also observed in the GPC cultures, which were deprived of systemic factors and other cell types, indicating that this is a cell autonomous phenomenon. Reduced size of the hypertrophic zone and decreased expression of the terminal hypertrophic chondrocyte marker *Opn*, as well as expansion of *Col2* expression to the chondro-osseous junction and absence of *Opn* expression within the hypertrophic zone, all suggest a delay in the terminal differentiation of chondrocytes in the absence of *Spry2*.

The *Spry2* gene product has been reported to be a negative regulator of RTK signaling, including the FGF pathway, in several contexts. SPRY2

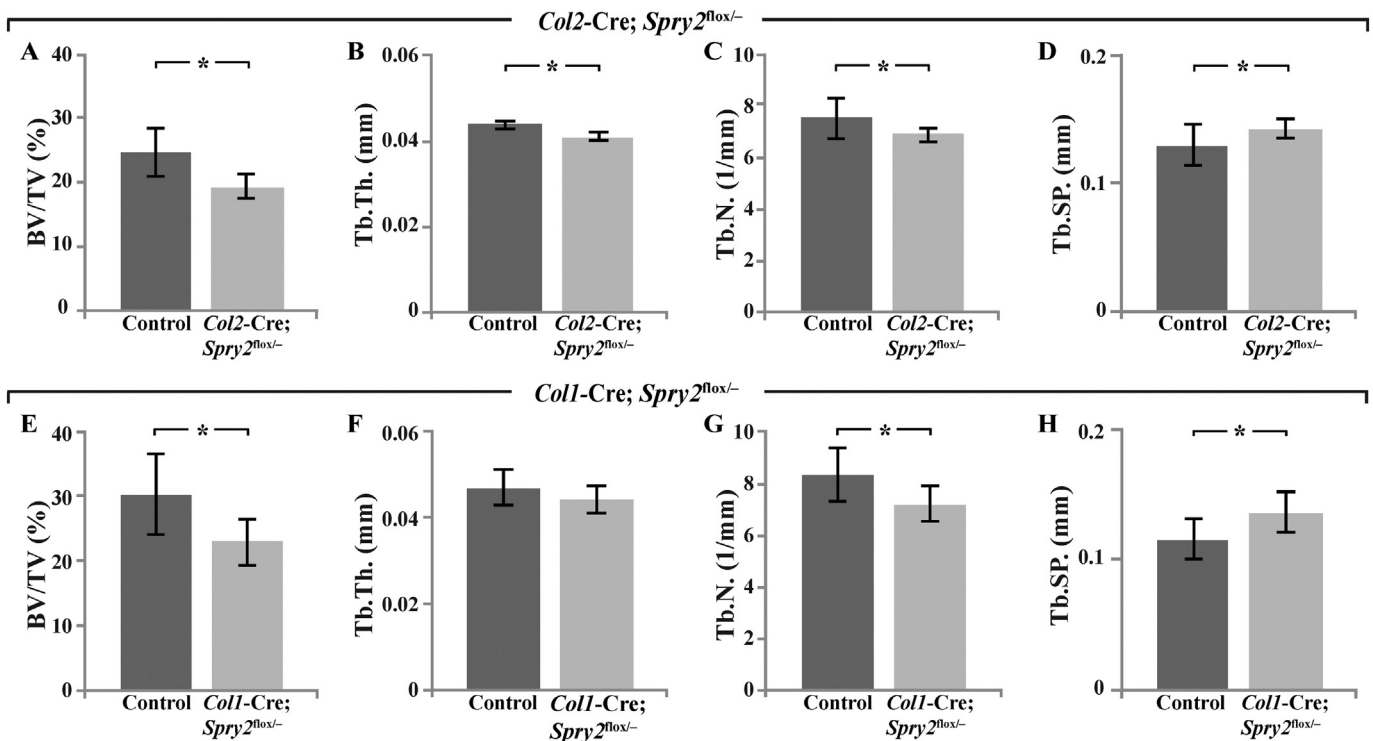


**Fig. 4.** Osteoblast- and chondrocyte-specific *Spry2* KO mice partly recapitulate Tb bone phenotype of the global *Spry2* null mice.  $\mu$ CT analyses of Tb bone in distal femurs of 6-week-old *Col2-Cre;Spry2<sup>lox/-</sup>* (A–D) and *Col1-Cre;Spry2<sup>lox/-</sup>* (E–H) show decreased BV/TV (A and E), Tb.Th. (B and F), and Tb.N (C and G) and increased Tb spacing (D and H) which are relatively milder (by  $\approx$  50%) than those in global *Spry2* KO mice. *Spry2<sup>lox/+</sup>* mice from the same litter were used as control. (\* $p < 0.05$ , \*\* $p < 0.005$ ).  $n = 8$  mice per genotype.

can inhibit FGF signaling by binding to GRB2 or RAF1 and preventing FGF-mediated MAPK activity [25,26]. Also, the *Fgfr3* missense mutant mice (*Fgfr-TDII*) have reduced proliferating chondrocytes with decreased *Ihh* and *ColX* expression [27] and the mutant gain-of-function phenotype is thought to be modulated by *Spry2* [28]. It was therefore surprising to find the opposite: a significant decrease in pMEK1/2 activity in *Spry2<sup>-/-</sup>* chondrocytes. It is possible that this could be due to a compensatory increase in the expression of *Spry1* and *Spry4* in chondrocytes; indeed, we have previously reported a compensatory up-regulation of *Spry1* in the absence of *Spry2* during tongue development [29]. However, we do not yet know whether *Spry1* or *Spry4*, or both, can compensate for the absence of *Spry2*, as any increased expression of *Spry1* and *Spry4* was insufficient to compensate for the inactivation of *Spry2*. This suggests that *Spry2* has other critical actions during endochondral bone formation beyond regulation of FGF signaling.

Indeed, we observed an upregulation of BMP signaling in *Spry2* KOs. These observations included increased *Bmp2* expression, decreased *Noggin* expression, and increased pSMAD1/5/8 activities in *Spry2<sup>-/-</sup>* GPCs. The increased *Ihh* expression and enhanced chondrocyte proliferation in *Spry2<sup>-/-</sup>* mice are consistent with increased BMP signaling, as previous studies showed that addition of BMP2 to limb cultures increased *Ihh* expression [30]. The delayed terminal differentiation of hypertrophic chondrocytes and decreased *Opn* expression are also compatible with increased BMP signaling in the *Spry2<sup>-/-</sup>* mice, as previous studies showed that blocking BMP signaling by chondrocyte-specific deletion of *Bmpr1a* led to increased expression of *Opn* and *Mmp13*, markers of terminal differentiation [23]. Additionally, treatment of embryonic limb cultures with *Noggin* increased *Opn* expression [30]. We were surprised to see that *PTHrP* expression was not markedly suppressed in the presence of *Ihh* upregulation in *Spry2<sup>-/-</sup>* GPs. One potential explanation for this observation is that more dense cartilage ECM, resulting from the increase in proliferating chondrocyte numbers, effectively blocked IHH diffusion to the perichondrium and caused disruption of *PTHrP* expression. Alternatively, deletion of *Spry2* could disrupt

signaling responses that are required to couple the PTHrP and *Ihh* pathways. Future studies will be needed to tease apart the detailed dynamics of these signaling interactions.

Analyses of postnatal *Spry2<sup>-/-</sup>* long bones revealed a reduced bone turnover, with concurrent decreases in bone formation and resorption. Overall, Tb bone mass was significantly decreased, likely due to impaired chondrocyte maturation. Hypertrophic chondrocytes are the key cells that induce osteogenesis; they synthesize ECM components and GFs to initiate vascularization of the GP, recruitment of osteogenic precursors, and calcification. Terminal hypertrophic chondrocytes at the chondro-osseous junction are marked by the expression of *Opn* and *Mmp-13* and the loss of *Col10* expression [23,31,32]. In late gestation *Spry2<sup>-/-</sup>* embryos, we observed high *Col10* expression within the hypertrophic zone that is similar to that of WT littermates, but a down-regulation of *Opn* expression at the chondro-osseous junction of the GP. Also, our preliminary data showed approximately 60% decrease in *Mmp13* and 40% decrease in alkaline phosphatase (*Ap*) mRNA levels when relative transcript levels were measured in both WT and *Spry2<sup>-/-</sup>* BMSC by qPCR (data not shown). Hence, these data indicate that without *Spry2* expression, terminal differentiation of hypertrophic chondrocytes is disrupted, which negatively affects bone formation. Furthermore, a decrease in OC activity seen in long bones of 6-week-old *Spry2<sup>-/-</sup>* mice could be due in part to reduced *Opn* expression within the ECM, as *Opn* is involved in the regulation of osteoclastic activities [33]. This is different from published *in vitro* data showing that BMP2 induces RANKL expression in hypertrophic chondrocytes to regulate osteoclastogenesis *in vitro* [34]. Complex interconnected molecular signaling pathways required for chondrogenesis might account for the discrepancy between our *in vivo* data and previously reported *in vitro* results, as loss of *Spry2* induced an increase in *Bmp2* expression sufficient to downregulate *Opn* expression, but not to affect RANKL expression.

The decrease in Tb bone in *Spry2<sup>-/-</sup>* mice was not exclusively due to impaired chondrocyte maturation. Osteoprogenitor cells from *Spry2<sup>-/-</sup>*

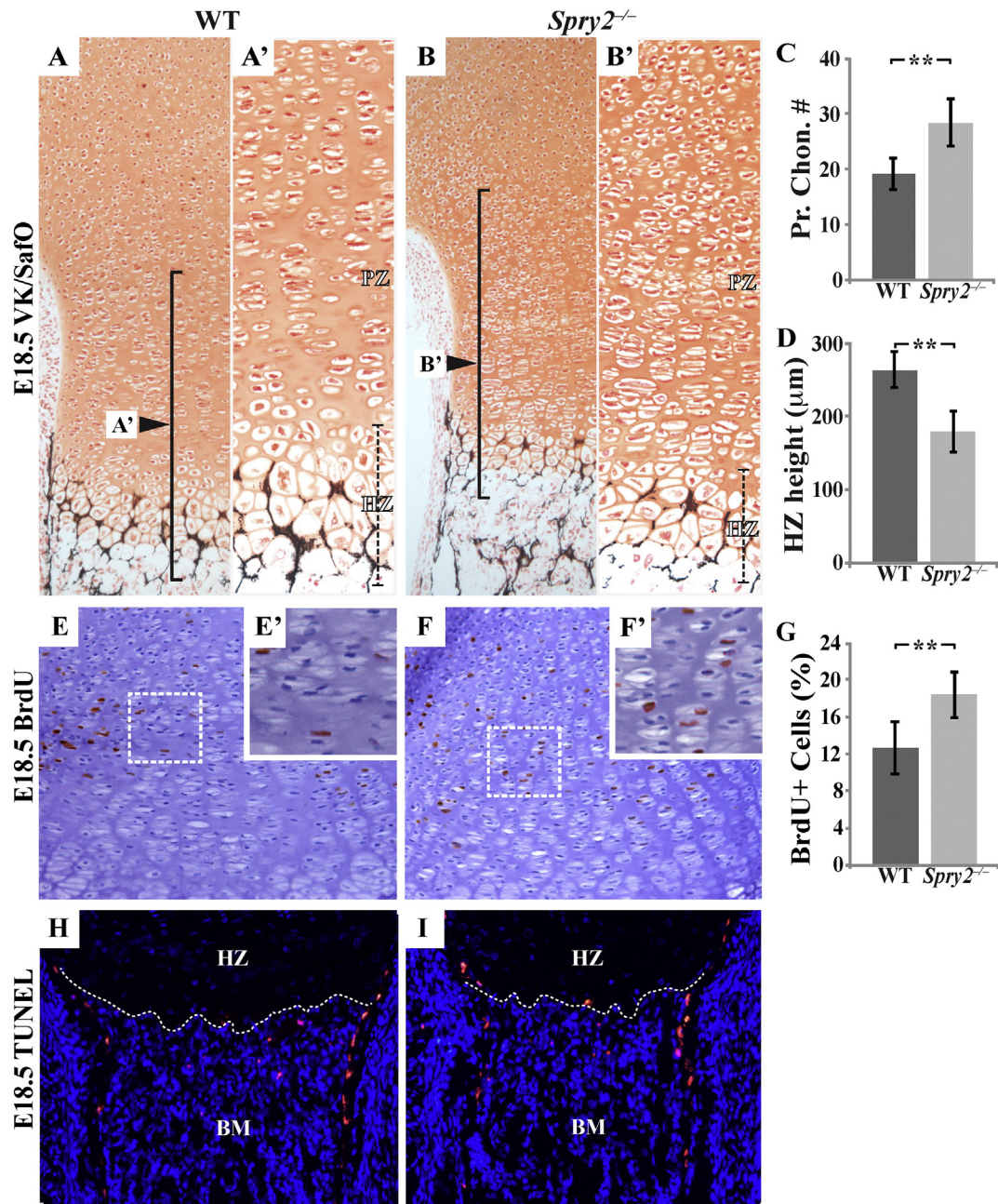


**Fig. 5.** *Spry2*<sup>-/-</sup> embryos have disrupted chondrogenesis due to increased proliferation. (A–B') VK/Safo staining of E18.5 femur sections shows there are more proliferating chondrocytes in the GP of *Spry2*<sup>-/-</sup> (B and B') than in that of WT (A and A'). Within the proliferative zone (PZ) of *Spry2*<sup>-/-</sup> embryos, a 32% increase in chondrocyte number is detected. (C,  $p < 0.001$ ) In addition, *Spry2*<sup>-/-</sup> embryos (B') have thinner hypertrophic zone (HZ; black dashed lines) than that of WT littermates (A'). Average height of the hypertrophic zone is decreased by 32% in *Spry2*<sup>-/-</sup> embryos (D,  $p < 0.001$ ). Measurements (unit = micrometer) are averaged and p values are calculated using the Student's t-test ( $*p < 0.05$ ,  $**p < 0.005$ ).  $n = 4$ /genotype. *Spry2*<sup>-/-</sup> embryos show elevated level of chondrocyte proliferation (E–F'), an increased number of BrdU-positive cells (brown-stained cells) by 34% (G,  $p < 0.001$ ).  $n = 3$ /genotype. Similar rates of apoptosis in WT and *Spry2*<sup>-/-</sup> embryos are demonstrated by similar numbers of TUNEL (red)-positive cells within the chondro-osseous junction (white dashed lines): HZ = hypertrophic zone, BM = bone marrow (H and I). (For interpretation of the references to color in this figure legend, the reader is referred to the web version of this article.)

mice had increased proliferation and impaired differentiation, similar to *Spry2*<sup>-/-</sup> chondrocytes. These findings indicate that *Spry2* has a role during OB differentiation in addition to its regulation of chondrogenesis. Furthermore,  $\mu$ CT analysis of *Col2-Cre;Spry2*<sup>fllox/-</sup> and *Col1-Cre;Spry2*<sup>fllox/-</sup> mice showed that both conditional KOs had a decrease in Tb.BV/TV that was approximately half that of *Spry2*<sup>-/-</sup> mice. Thus, the *Spry2*<sup>-/-</sup> skeletal phenotype was due to defects in both chondrocyte and OB function.

The mechanism that causes upregulation of *Bmp2* in *Spry2*<sup>-/-</sup> mice is not clear, since the role of *Spry2* in regulating the expression of *Bmps* or in BMP signaling is not known. Also, we cannot rule out the possibility of

signaling pathways other than BMP or RTK being affected by the inactivation of *Spry2*. However, our data suggest that SPRY2 interacts with both FGF and BMP signaling pathways to control chondrocyte development. Loss of *Spry2* causes upregulation of *Spry1* and *Spry4* expression, which leads to suppression of FGF signaling. Either through this suppression of RTK signaling or through loss of a negative effect of *Spry2* directly on the BMP signaling pathway, BMP signaling is subsequently increased, which manifests as upregulated *Ihh* expression, increased chondrocyte proliferation, and impaired terminal chondrocyte differentiation. Together, our data show that *Spry2* is important for normal chondrocyte proliferation and differentiation, and loss of *Spry2* leads to defects in

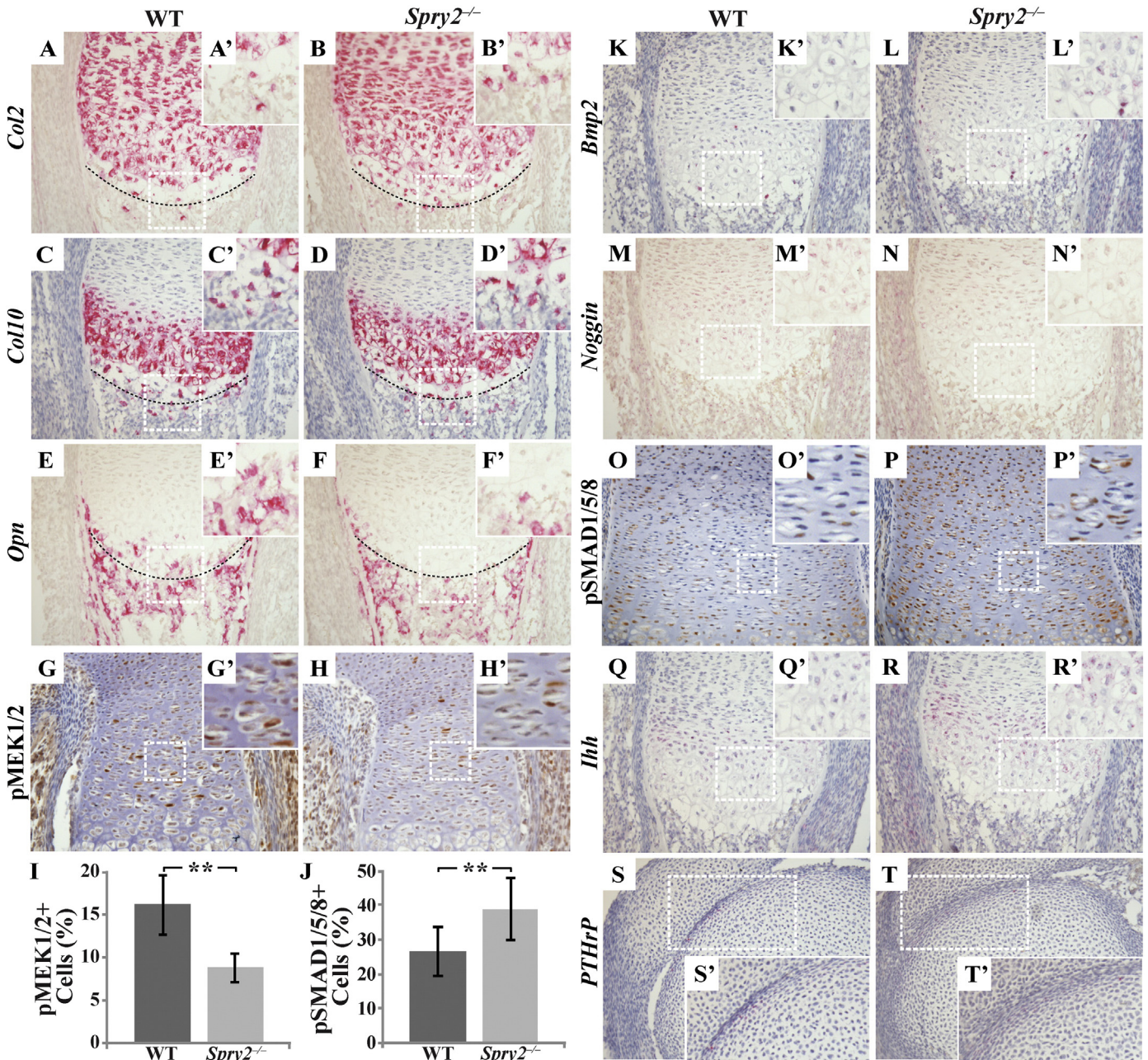


**Fig. 6.** Deletion of *Spry2* leads to increased BMP signaling and decreased RTK signaling during chondrogenesis. RNAscope assay shows changes in expression levels of molecular markers for different stages of chondrogenesis in femur sections from E16.5 *Spry2*<sup>-/-</sup> embryos (A–F', K–N', Q–T'). Immunohistochemical staining for pMEK1/2 (G–H') and pSMAD1/5/8 (O–P') reveals a decrease in the number of pMEK1/2-positive cells ( $^{*}p < 0.001$ ), but an increase in pSMAD1/5/8-positive cells ( $^{**}p < 0.001$ ) in *Spry2*<sup>-/-</sup> embryos. In *Spry2*<sup>-/-</sup> samples, more *Col2*-expressing cells are found extending to the chondro-osseous junction (B and B'). Also, *Opn* expression is only detected in primary spongiosa of *Spry2*<sup>-/-</sup> (F and F') while in WT, *Opn* expression starts from hypertrophic zone (E and E'). *Noggin* (M–N') expression is decreased while expression of *Bmp* (K–L') and *Ihh* (Q–R') is increased in *Spry2*<sup>-/-</sup>. The *PTHrP* expression seems similar to that of WT control (S–T'). Magnification = 200 $\times$ .

endochondral bone formation and bone mass accrual, likely due to an up-regulation of BMP signaling. The Tb bone mass defect is further influenced by the role of *Spry2* in OB differentiation and function.

Supplementary data to this article can be found online at <http://dx.doi.org/10.1016/j.bone.2016.04.023>.

#### Disclosure

All authors state that they have no conflicts of interest.

#### Acknowledgments

We thank Dong-Kha Tran, Sarah Alto, Rebecca D'Urso, and Asoka Rathnayake for technical assistance, Wei-Dar Lu and Tsui-Hua Chen for the calvarial OB primary culture system, and the SF-VAMC Bone Imaging Core facilities for help with  $\mu$ CT scans and histomorphometric analyses. We also thank Dr. Amnon Sharir for his review of the manuscript and helpful comments. This work was supported by NIH T32 DE007306 to AJ, R03AR057121 and R01DE024988 to ODK and R01AR067291 and P30AR066262 to WC.

Authors' roles: Study design: AJ, RL, WC, and ODK. Study conduct: AJ, RL, ZC, and WC. Data collection: AJ, RL, ZC, CA, and WC. Data analysis: AJ, RL, ZC, WC, and ODK. Data interpretation: AJ, RL, WC, and ODK. Draft manuscript: AJ and RL. Revising manuscript content: AJ, RL, WC, and ODK. Approving final version of manuscript: AJ, RL, CA, WC, and ODK. ODK takes responsibility for the integrity of the data analysis.

## References

- [1] H.M. Kronenberg, Developmental regulation of the growth plate, *Nature* 423 (6937) (2003 May 15) 332–336 PubMed PMID: 12748651. eng.
- [2] E.J. Mackie, L. Tatarczuch, M. Mirams, The skeleton: a multi-functional complex organ: the growth plate chondrocyte and endochondral ossification, *J. Endocrinol.* 211 (2) (2011 Nov) 109–121 PubMed PMID: 21642379. (Epub 2011/06/07. eng).
- [3] N. Hacohen, S. Kramer, D. Sutherland, Y. Hiroimi, M.A. Krasnow, Sprouty encodes a novel antagonist of FGF signaling that patterns apical branching of the Drosophila airways, *Cell* 92 (2) (1998 Jan 23) 253–263 PubMed PMID: 9458049.
- [4] G. Minowada, L.A. Jarvis, C.L. Chi, A. Neubuser, X. Sun, N. Hacohen, et al., Vertebrate sprouty genes are induced by FGF signaling and can cause chondrodysplasia when overexpressed, *Development* 126 (20) (1999 Oct) 4465–4475 PubMed PMID: 10498682. (Epub 1999/09/28. eng).
- [5] J.D. Tefft, M. Lee, S. Smith, M. Leinwand, J. Zhao, P. Bringas Jr., et al., Conserved function of mSpry-2, a murine homolog of Drosophila sprouty, which negatively modulates respiratory organogenesis, *Curr. Biol.* 9 (4) (1999 Feb 25) 219–222 PubMed PMID: 10074434. (Epub 1999/03/13. eng).
- [6] A.A. de Maximy, Y. Nakatake, S. Moncada, N. Itoh, J.P. Thiery, S. Bellusci, Cloning and expression pattern of a mouse homologue of Drosophila sprouty in the mouse embryo, *Mech. Dev.* 81 (1–2) (1999 Mar) 213–216 PubMed PMID: 10330503.
- [7] M.A. Impagnatiello, S. Weitzer, G. Gannon, A. Compagni, M. Cotten, G. Christofori, Mammalian sprouty-1 and -2 are membrane-anchored phosphoprotein inhibitors of growth factor signaling in endothelial cells, *J. Cell Biol.* 152 (5) (2001 Mar 5) 1087–1098 PubMed PMID: 11238463.
- [8] M. Kajita, W. Ikeda, Y. Tamaru, Y. Takai, Regulation of platelet-derived growth factor-induced Ras signaling by poliovirus receptor Necl-5 and negative growth regulator Sprouty2, *Genes Cells* 12 (3) (2007 Mar) 345–357 PubMed PMID: 17352739. (Epub 2007/03/14. eng).
- [9] J.E. Egan, A.B. Hall, B.A. Yatsula, D. Bar-Sagi, The bimodal regulation of epidermal growth factor signaling by human sprouty proteins, *Proc. Natl. Acad. Sci. U. S. A.* 99 (9) (2002 Apr 30) 6041–6046 PubMed PMID: 11983899.
- [10] O.D. Klein, G. Minowada, R. Peterkova, A. Kangas, B.D. Yu, H. Lesot, et al., Sprouty genes control diastema tooth development via bidirectional antagonism of epithelial–mesenchymal FGF signaling, *Dev. Cell* 11 (2) (2006 Aug) 181–190 PubMed PMID: 16890158. Pubmed Central PMCID: 2847684. (Epub 2006/08/08. eng).
- [11] L. Chi, S. Zhang, Y. Lin, R. Prunskaitė-Hyyryläinen, R. Vuolteenaho, P. Itaranta, et al., Sprouty proteins regulate ureteric branching by coordinating reciprocal epithelial Wnt1, mesenchymal Gdnf and stromal Fgf7 signalling during kidney development, *Development* 131 (14) (2004 Jul) 3345–3356 PubMed PMID: 15201220. (Epub 2004/06/18. eng).
- [12] E. Minina, C. Kreschel, M.C. Naski, D.M. Ornitz, A. Vortkamp, Interaction of FGF, Ihh/Pthlh, and BMP signaling integrates chondrocyte proliferation and hypertrophic differentiation, *Dev. Cell* 3 (3) (2002 Sep) 439–449 PubMed PMID: 12361605. eng.
- [13] D.M. Ornitz, FGF signaling in the developing endochondral skeleton, *Cytokine Growth Factor Rev.* 16 (2) (2005 Apr) 205–213 PubMed PMID: 15863035. Pubmed Central PMCID: 3083241. (Epub 2005/05/03. eng).
- [14] M.A. Basson, S. Akbulut, J. Watson-Johnson, R. Simon, T.J. Carroll, R. Shakya, et al., Sprouty1 is a critical regulator of GDNF/RET-mediated kidney induction, *Dev. Cell* 8 (2) (2005 Feb) 229–239 PubMed PMID: 15691764. eng.
- [15] K. Shim, G. Minowada, D.E. Coling, G.R. Martin, Sprouty2, a mouse deafness gene, regulates cell fate decisions in the auditory sensory epithelium by antagonizing FGF signaling, *Dev. Cell* 8 (4) (2005 Apr) 553–564 PubMed PMID: 15809037.
- [16] F. Liu, H.W. Woitge, A. Braut, M.S. Kronenberg, A.C. Lichtler, M. Mina, et al., Expression and activity of osteoblast-targeted Cre recombinase transgenes in murine skeletal tissues, *Int. J. Dev. Biol.* 48 (7) (2004 Sep) 645–653 PubMed PMID: 15470637.
- [17] D.A. Ovchinnikov, J.M. Deng, G. Ogunrinu, R.R. Behringer, Col2a1-directed expression of Cre recombinase in differentiating chondrocytes in transgenic mice, *Genesis* 26 (2) (2000 Feb) 145–146 PubMed PMID: 10686612.
- [18] L. Rodriguez, C. Tu, Z. Cheng, T.H. Chen, D. Bikle, D. Shoback, et al., Expression and functional assessment of an alternatively spliced extracellular Ca<sup>2+</sup> –sensing receptor in growth plate chondrocytes, *Endocrinology* 146 (12) (2005 Dec) 5294–5303 PubMed PMID: 16166224. (Epub 2005/09/17. eng).
- [19] Y. Wang, S. Nishida, B.M. Boudignon, A. Burghardt, H.Z. Elalieh, M.M. Hamilton, et al., IGF-1 receptor is required for the anabolic actions of parathyroid hormone on bone, *J. Bone Miner. Res. Off. J. Am. Soc. Bone Miner. Res.* 22 (9) (2007 Sep) 1329–1337 PubMed PMID: 17539737. (Epub 2007/06/02. eng).
- [20] M.L. Boussein, S.K. Boyd, B.A. Christiansen, R.E. Guldberg, K.J. Jepsen, R. Muller, Guidelines for assessment of bone microstructure in rodents using micro-computed tomography, *J. Bone Miner. Res. Off. J. Am. Soc. Bone Miner. Res.* 25 (7) (2010 Jul) 1468–1486 PubMed PMID: 20533309. (Epub 2010/06/10).
- [21] D.W. Dempster, J.E. Compston, M.K. Drezner, F.H. Glorieux, J.A. Kanis, H. Malluche, et al., Standardized nomenclature, symbols, and units for bone histomorphometry: a 2012 update of the report of the ASBMR Histomorphometry Nomenclature Committee, *J. Bone Miner. Res. Off. J. Am. Soc. Bone Miner. Res.* 28 (1) (2013 Jan) 2–17 PubMed PMID: 23197339. (Epub 2012/12/01. eng).
- [22] K.N. Retting, B. Song, B.S. Yoon, K.M. Lyons, BMP canonical Smad signaling through Smad1 and Smad5 is required for endochondral bone formation, *Development* 136 (7) (2009 Apr) 1093–1104 PubMed PMID: 19224984. Pubmed Central PMCID: 2668702. (Epub 2009/02/20. eng).
- [23] B.S. Yoon, R. Pogue, D.A. Ovchinnikov, I. Yoshii, Y. Mishina, R.R. Behringer, et al., BMPs regulate multiple aspects of growth-plate chondrogenesis through opposing actions on FGF pathways, *Development* 133 (23) (2006 Dec) 4667–4678 PubMed PMID: 17065231. eng.
- [24] P. Purcell, A. Jheon, M.P. Vivero, H. Rahimi, A. Joo, O.D. Klein, Spry1 and spry2 are essential for development of the temporomandibular joint, *J. Dent. Res.* 91 (4) (2012 Apr) 387–393 PubMed PMID: 22328578. Pubmed Central PMCID: 3310757. (Epub 2012/02/14. eng).
- [25] H. Hanafusa, S. Torii, T. Yasunaga, E. Nishida, Sprouty1 and Sprouty2 provide a control mechanism for the Ras/MAPK signalling pathway, *Nat. Cell Biol.* 4 (11) (2002 Nov) 850–858 PubMed PMID: 12402043. (Epub 2002/10/29. eng).
- [26] P. Yusoff, D.H. Lao, S.H. Ong, E.S. Wong, J. Lim, T.L. Lo, et al., Sprouty2 inhibits the Ras/MAP kinase pathway by inhibiting the activation of Raf, *J. Biol. Chem.* 277 (5) (2002 Feb 1) 3195–3201 PubMed PMID: 11698404. (Epub 2001/11/08. eng).
- [27] C. Li, L. Chen, T. Iwata, M. Kitagawa, X.Y. Fu, C.X. Deng, A Lys644Glu substitution in fibroblast growth factor receptor 3 (FGFR3) causes dwarfism in mice by activation of STATs and ink4 cell cycle inhibitors, *Hum. Mol. Genet.* 8 (1) (1999 Jan) 35–44 PubMed PMID: 9887329.
- [28] C. Guo, C.R. Degnin, M.B. Laederich, G.P. Lunstrum, P. Holden, J. Bihlmaier, et al., Sprouty 2 disturbs FGFR3 degradation in thanatophoric dysplasia type II: a severe form of human achondroplasia, *Cell. Signal.* 20 (8) (2008 Aug) 1471–1477 PubMed PMID: 18485666. Pubmed Central PMCID: PMC2675614.
- [29] C.I. Petersen, A.H. Jheon, P. Mostowfi, C. Charles, S. Ching, S. Thirumangalathu, et al., FGF signaling regulates the number of posterior taste papillae by controlling progenitor field size, *PLoS Genet.* 7 (6) (2011 Jun) e1002098 PubMed PMID: 21655085. Pubmed Central PMCID: 3107195. (Epub 2011/06/10. eng).
- [30] E. Minina, H.M. Wenzel, C. Kreschel, S. Karp, W. Gaffield, A.P. McMahon, et al., BMP and Ihh/PThrP signaling interact to coordinate chondrocyte proliferation and differentiation, *Development* 128 (22) (2001 Nov) 4523–4534 PubMed PMID: 11714677. (Epub 2001/11/21. eng).
- [31] C.W. Wu, E.V. Tchertina, F. Mwale, K. Hasty, I. Pidoux, A. Reiner, et al., Proteolysis involving matrix metalloproteinase 13 (collagenase-3) is required for chondrocyte differentiation that is associated with matrix mineralization, *J. Bone Miner. Res. Off. J. Am. Soc. Bone Miner. Res.* 17 (4) (2002 Apr) 639–651 PubMed PMID: 11918221. (Epub 2002/03/29).
- [32] E. Kozhemyakina, A.B. Lassar, E. Zelzer, A pathway to bone: signaling molecules and transcription factors involved in chondrocyte development and maturation, *Development* 142 (5) (2015 Mar 1) 817–831 PubMed PMID: 25715393. Pubmed Central PMCID: 4352987. (Epub 2015/02/26).
- [33] A. Franzen, K. Hulthenby, F.P. Reinholt, P. Onnerfjord, D. Heinegard, Altered osteoclast development and function in osteopontin deficient mice, *J. Orthop. Res.* 26 (5) (2008 May) 721–728 PubMed PMID: 18050311. (Epub 2007/12/01. eng).
- [34] M. Usui, L. Xing, H. Drissi, M. Zuscik, R. O'Keefe, D. Chen, et al., Murine and chicken chondrocytes regulate osteoclastogenesis by producing RANKL in response to BMP2, *J. Bone Miner. Res. Off. J. Am. Soc. Bone Miner. Res.* 23 (3) (2008 Mar) 314–325 PubMed PMID: 17967138. Pubmed Central PMCID: PMC2636701.